

# Highly efficient femtosecond pulse stretching by tailoring cavity dispersion in erbium fiber lasers with an intracavity short-pass edge filter

Nan-Kuang Chen,<sup>1,2,\*</sup> Feng-Zhou Liu,<sup>1</sup> Hsiu-Po Chuang,<sup>3</sup> Yinchieh Lai,<sup>4</sup> Shang-Da Yang,<sup>3</sup> Jim-Wein Lin,<sup>3</sup> Shien-Kuei Liaw,<sup>5</sup> Yu-Chung Chang,<sup>6</sup> Chen-Bin Huang,<sup>3</sup> and Sien Chi<sup>4,7</sup>

<sup>1</sup>Department of Electro-Optical Engineering, National United University, Miaoli, 360, Taiwan

<sup>2</sup>Optoelectronics Research Center, National United University, Miaoli, 360, Taiwan

<sup>3</sup>Institute of Photonics Technologies, National Tsing Hua University, Hsinchu, 300, Taiwan

<sup>4</sup>Department of Photonics, National Chiao Tung University, Hsinchu, 300, Taiwan

<sup>5</sup>Graduate Institute of Electro-Optical Engineering, National Taiwan University of Science and Technology, Taipei, 106, Taiwan

<sup>6</sup>Department of Electrical Engineering, National Changhua University of Education, Changhua, 500, Taiwan

<sup>7</sup>Department of Photonic Engineering, Yuan Ze University, Chungli, 320, Taiwan

\*nkchen@nuu.edu.tw

**Abstract:** We demonstrate highly efficient pulse stretching in Er<sup>3+</sup>-doped femtosecond mode-locked fiber lasers by tailoring cavity dispersion using an intracavity short-pass edge filter. The cavity dispersion is preset at around zero to obtain the shortest pulsewidth. When the cutoff wavelength of the short-pass edge filter is thermo-optically tuned to overlap the constituting spectral components of mode-locked pulses, large negative waveguide dispersion is introduced by the steep cutoff slope and the total cavity dispersion is moved to normal dispersion regime to broaden the pulsewidth. The time-bandwidth product of the mode-locked pulse increases with the decreasing temperature at the optical liquid surrounding the short-pass edge filter. Pulse stretch ratio of 3.53 (623.8fs/176.8fs) can be efficiently achieved under a temperature variation of 4°C.

©2011 Optical Society of America

**OCIS codes:** (060.2340) Fiber optics components; (140.4050) Mode-locked lasers; (230.2035) Dispersion compensation devices.

---

## References and links

1. N. Nishizawa, Y. Chen, P. Hsiung, E. P. Ippen, and J. G. Fujimoto, "Real-time, ultrahigh-resolution, optical coherence tomography with an all-fiber, femtosecond fiber laser continuum at 1.5 microm," *Opt. Lett.* **29**(24), 2846–2848 (2004).
2. D. I. Yeom, E. C. Mägi, M. R. E. Lamont, M. A. F. Roelens, L. Fu, and B. J. Eggleton, "Low-threshold supercontinuum generation in highly nonlinear chalcogenide nanowires," *Opt. Lett.* **33**(7), 660–662 (2008).
3. Y. Zhao, Y. Liang, N. Zhang, M. Wang, and X. Zhu, "Pulse width effect in ultrafast laser ionization imaging," *Opt. Lett.* **33**(21), 2467–2469 (2008).
4. F. Röser, T. Eidam, J. Rothhardt, O. Schmidt, D. N. Schimpf, J. Limpert, and A. Tünnermann, "Millijoule pulse energy high repetition rate femtosecond fiber chirped-pulse amplification system," *Opt. Lett.* **32**(24), 3495–3497 (2007).
5. A. Chong, W. H. Renninger, and F. W. Wise, "Properties of normal-dispersion femtosecond fiber lasers," *J. Opt. Soc. Am. B* **25**(2), 140–148 (2008).
6. V. P. Kalosha, L. Chen, and X. Bao, "Ultra-short pulse operation of all-optical fiber passively mode-locked ytterbium laser," *Opt. Express* **14**(11), 4935–4945 (2006).
7. M. E. Fermann, K. Sugden, and I. Bennion, "High-power soliton fiber laser based on pulse width control with chirped fiber Bragg gratings," *Opt. Lett.* **20**(2), 172–174 (1995).
8. F. Haxsen, D. Wandt, U. Morgner, J. Neumann, and D. Kracht, "Pulse characteristics of a passively mode-locked thulium fiber laser with positive and negative cavity dispersion," *Opt. Express* **18**(18), 18981–18988 (2010).
9. H. A. Haus, J. G. Fujimoto, and E. P. Ippen, "Structures for additive pulse mode locking," *J. Opt. Soc. Am. B* **8**(10), 2068–2076 (1991).
10. N. K. Chen, C. M. Hung, S. Chi, and Y. Lai, "Towards the short-wavelength limit lasing at 1450 nm over <sup>4</sup>I<sub>13/2</sub>→<sup>4</sup>I<sub>15/2</sub> transition in silica-based erbium-doped fiber," *Opt. Express* **15**(25), 16448–16456 (2007).

11. N. K. Chen, K. C. Hsu, S. K. Liaw, Y. Lai, and S. Chi, "Influence of depressed-index outer ring on evanescent tunneling loss in tapered double-cladding fibers," *Opt. Lett.* **33**(15), 1666–1668 (2008).
12. A. M. Vengsarkar and W. A. Reed, "Dispersion-compensating single-mode fibers: efficient designs for first- and second-order compensation," *Opt. Lett.* **18**(11), 924–926 (1993).
13. C. D. Poole, J. M. Weisenfeld, D. J. DiGiovanni, and A. M. Vengsarkar, "Optical fiber-based dispersion compensation using higher order modes near cutoff," *J. Lightwave Technol.* **12**(10), 1746–1758 (1994).
14. R. Zhang, J. Teipel, X. Zhang, D. Nau, and H. Giessen, "Group velocity dispersion of tapered fibers immersed in different liquids," *Opt. Express* **12**(8), 1700–1707 (2004).
15. M. Rusu, R. Herda, S. Kivistö, and O. G. Okhotnikov, "Fiber taper for dispersion management in a mode-locked ytterbium fiber laser," *Opt. Lett.* **31**(15), 2257–2259 (2006).
16. E. Ding, S. Lefrancois, J. N. Kutz, and F. W. Wise, "Scaling fiber lasers to large mode area: an investigation of passive mode-locking using a multi-mode fiber," *IEEE Photon. Technol. Lett.* **47**(5), 597–606 (2011).
17. N. K. Chen, S. Chi, and S. M. Tseng, "Wideband tunable fiber short-pass filter based on side-polished fiber with dispersive polymer overlay," *Opt. Lett.* **29**(19), 2219–2221 (2004).
18. H. P. Chuang and C. B. Huang, "Generation and delivery of 1-ps optical pulses with ultrahigh repetition-rates over 25-km single mode fiber by a spectral line-by-line pulse shaper," *Opt. Express* **18**(23), 24003–24011 (2010).
19. Y. F. Chen, S. W. Tsai, S. C. Wang, and J. Chen, "A diode-pumped high power Q-switched and self-mode-locked Nd:YVO<sub>4</sub> laser with a LiF: F<sub>2</sub><sup>-</sup> saturable absorber," *Appl. Phys. B* **73**, 115–118 (2001).

---

## 1. Introduction

Femtosecond mode-locked fiber lasers (FMLLs) have played important roles in optical coherence tomography imaging, supercontinuum generation, precision sensing, micro/nano-machining, micro/nano-surgery, time resolved spectroscopy, chemical/biological reaction triggering/monitoring, and high speed fiber-optic communications [1,2]. From the viewpoint of material processing, femtosecond fiber lasers are useful in generating micro-holes with sharp cutting edge due to less thermal-diffusion effect and the shorter lasing wavelength when compared with CO<sub>2</sub> lasers. Moreover, fiber lasers are also featured with high peak power, excellent beam quality, low thermal load, strong power confinement, long interaction length, and ultra-short pulses through the mode-locking effects. The mode-locked fiber laser pulses can give rise to a very high peak power when the cavity dispersion and polarization effects are well controlled. In practical applications, the pulse intensity capable of easy, fast, and wide-range tuning is important when a composite material is targeted in a micromachining or in a direct-writing process [3]. An efficient way to quickly change the laser peak intensity is to change the laser pulsewidth instead. For stationary pulse energy, a wider laser pulsewidth can lead to a lower laser peak power because the pulsewidth times the peak power equals to the pulse energy. In addition to peak intensity tuning, a pulse stretchable FMLL is also advantageous for precision sensing system of varying sensing distance and resolution, like optical time-domain reflectometer (OTDR). As well, the pulse stretching is one of the necessary steps for chirped pulse amplification (CPA) [4] and for high pulse energy mode-locked fiber lasers at extremely large normal dispersion [5]. Since the mode-locked pulses can be stretched or compressed by adjusting the cavity length or by introducing chirped gratings and filters [6–8] to change the cavity dispersion and Kerr nonlinearity, the laser peak power can thus be tuned to a desired value. However, the FMLL with a widely tunable pulsewidth is difficult to achieve because an extra dispersion compensation fiber with a tightly precise length for cavity dispersion adjustment is usually required to obtain a desired pulsewidth [6]. It lacks of flexibility and reproducibility in terms of tunability. On the other hand, Bragg grating is expensive and is not widely wavelength tunable.

Based on the above observation, in this work, we demonstrate an efficient pulse stretchable Er<sup>3+</sup>-doped FMLL, operating in a polarization additive-pulse mode-locking configuration [9], by dispersionally stretching the mode-locked pulses. To facilitate the pulse stretching, the cavity dispersion of FMLL is intentionally tuned to close to the zero but still in the anomalous dispersion regime. The cavity dispersion and the Kerr nonlinearity are balanced and a shortest pulsewidth can be obtained. The pulse stretching is further achieved by incorporating a widely tunable fiber short-pass edge filter (SPEF) with a steep cutoff edge into the laser cavity, as shown in Fig. 1(a). The SPEF had been employed in achieving tunable CW fiber lasers as well as S-band erbium-doped fiber amplifiers by discretely suppressing the

long-wavelength amplified spontaneous emission (ASE) noises [10,11]. The SPEF has a steep cutoff slope, as shown in Fig. 1(b), due to the material dispersion discrepancy between the silica core and liquid cladding materials [10,11]. The spectral characteristics become highly wavelength-dependent near the cutoff, which generates large negative waveguide dispersion (ps/nm/km). Thus, the waveguide dispersion of this highly dispersive composite waveguide structure is very strong compared with the material dispersion and the net cavity dispersion of FMLL is moved to normal dispersion regime to cause pulse stretching for mode-locked pulses. A fast switching between the shallow anomalous dispersion and deep normal dispersion regime is crucial to an efficient pulse stretching in FMLL. Consequently, a large negative dispersion must be rapidly and dynamically introduced into laser cavity. It is known that a large negative dispersion comes from the rapid power change from the core to the cladding [12,13] and can be available near the fundamental-mode ( $LP_{01}$  mode) cutoff wavelength in an optical fiber with a depressed-index inner cladding [12] or near the second-mode ( $LP_{11}$  mode) cutoff wavelength in multimode fiber [13]. Based on dispersion engineering technique through selecting suitable composite materials and waveguide structures in tapered fibers, a large negative dispersion [14] or a large positive dispersion [15] can be achieved. Accordingly, the SPEF can provide large negative dispersion near the cutoff wavelength. In the beginning, the cavity dispersion of fiber laser is preset around zero to obtain the shortest pulsewidth of  $\sim 176.8$  fs. When the cutoff wavelength of intracavity SPEF is thermo-optically tuned to overlap the long-wavelength components of mode-locked pulses, the large negative waveguide dispersion is introduced into the laser cavity to broaden the mode-locked pulse. The pulse can be stretched from 176.8fs to 623.8fs (total pulsewidth stretching of 447fs) under a temperature variation of  $4^\circ\text{C}$  (from  $36^\circ\text{C}$  to  $32^\circ\text{C}$ ) at the SPEF. This high efficient pulse-stretching scheme based on tunable waveguide dispersion is easier than changing the corresponding fiber length in laser cavity. It could also be promising for the high power stretched-pulse additive mode-locking lasers since the longer pulse duration, compared with the shorter pulse duration in soliton laser, can support much higher pulse energies before the Kerr nonlinearity is growing strong to cause multi-pulsing instability [16] or to damage the host glass material.

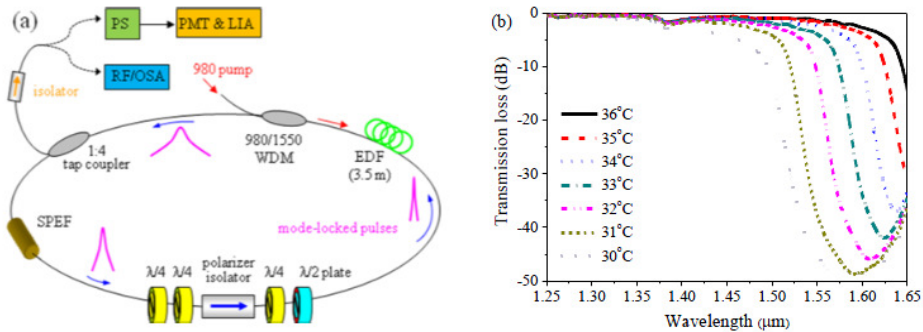


Fig. 1. (a) Experimental set-up of our pulse-stretchable  $\text{Er}^{3+}$ -doped mode-locked fiber laser. WDM: wavelength division multiplexer, OSA: optical spectrum analyzer, RF: RF spectrum analyzer, AC: autocorrelator, SPEF: short-pass edge filter, EDF: erbium-doped fiber, PS: pulse shaper, PMT: photomultiplier tube, LIA: lock-in amplifier. (b) Spectral responses of a SPEF with an optical liquid ( $n_D = 1.456$ ) at different heating temperatures. (Res: 1 nm).

## 2. Fabrication and experiments

Figure 1(a) shows the experimental setup of the FMLL. The operation of the FMLL is based on polarization additive pulse mode-locking. A 3.5-m-long EDF (OFS: R37005) with a positive group velocity dispersion (GVD) parameter  $\beta_2$  is used as the gain medium whereas the single-mode fiber (Corning: SMF-28) has a negative  $\beta_2$  of about  $-20 \text{ ps}^2/\text{km}$  at  $1.55 \mu\text{m}$  wavelength. The cavity dispersion is fine tuned by using a section of SMF-28 with proper length to make the net cavity dispersion in the anomalous dispersion regime but is quite close

to the zero GVD. The polarization controller is used to generate the elliptically polarized light in the resonator. The horizontal and vertical components of the elliptically polarized light will suffer different nonlinear phase shifts, which leads to nonlinear polarization rotation. The nonlinear optical phenomenon comes from the nonlinear Kerr effect in fiber. Accordingly, the laser amplitude will be modulated at an extremely fast speed when the rotary polarization passing through a polarization-dependent isolator which actually plays as a saturable absorber in resonator. The FMLL based on the nonlinear polarization rotation method is called polarization additive pulse mode-locking [9] and is the working principle of our FMLL. In order to tailor the cavity dispersion to enable the FMLL operating in the stretched-pulse regime for pulse stretching, a SPEF capable of providing large negative waveguide dispersion is implemented into the cavity between the output coupler and the waveplates, as shown in Fig. 1(a). It is known that a rapid power variation with wavelength from the core to the cladding can give rise to large negative waveguide dispersion [12]. When more optical powers quickly move into the cladding from the core, the group index and the group delay rapidly decreases with wavelength. Accordingly, the waveguide dispersion becomes highly negative when the wavelength is closing to a sharp fundamental-mode cutoff [10,11] since the optical powers move to the outside from the tapered fiber abruptly. To design a SPEF with a sharp cutoff, the material dispersion discrepancy between the tapered fiber and the surrounding optical liquid must be carefully selected [10]. The waveguide dispersion is also crucial to enhance the steepness of the fundamental-mode cutoff [11]. Since the thermo-optic coefficient of the Cargille<sup>®</sup> index liquid is high, the cutoff wavelength can be efficiently tunable [10,11]. Thus, it is advantageous to produce the wavelength-tunable large negative waveguide dispersion to tailor the cavity dispersion of FMLL for pulse stretching in a controlled manner.

In fabrication, the SMF-28 was heated and stretched using a scanning hydrogen flame fiber-tapering workstation until the diameter of tapered waist is approaching 30  $\mu\text{m}$ . The length of uniform waist is about 1.5 cm and is crucial to the cutoff slope [10]. The tapered fiber was then glued into a U-groove engraved on a glass substrate and an optical dispersive Cargille<sup>®</sup> index liquid ( $n_D = 1.456$ ) was used to surround the tapered region. Since the silica tapered fiber has a higher dispersion slope than that of the Cargille index liquid, their refractive index dispersion curves will cross each other at a cutoff point [10,11]. This point separates the stopband and passband wavelengths and can be movable when the index liquid is heating up or cooling down by a thermoelectric cooler (TE-cooler). The tapered waist diameter was intentionally selected to be around 30  $\mu\text{m}$  to obtain the steepest cutoff slope as well as the largest attenuation for stopband, so that the large negative waveguide dispersion can be introduced into FMLL to stretch the mode-locked pulses. The SPEF so made can be tuning over 1250-1650 nm with the rejection efficiency above 45 dB and the cutoff slope of higher than  $-1.0$  dB/nm. The spectral responses, measured by an optical spectrum analyzer (OSA) under the resolution (RES) of 1 nm, within the temperature variation of 6  $^{\circ}\text{C}$  (30-36 $^{\circ}\text{C}$ ) are shown in Fig. 1(b). The controlled temperature was stabilized to within 0.1 $^{\circ}\text{C}$  accuracy by a dual TE-cooler module and the cutoff wavelength can be tuned at a speed of a few tens of milliseconds for 1 nm wavelength-shift while the spectral shape is always the same [17]. This widely tunable SPEF was subsequently incorporated into an Er<sup>3+</sup>-doped FMLL, as shown in Fig. 1(a), to serve as the pulse stretcher when the polarization controller and the cavity dispersion are correctly controlled. A reflective 4-f pulse shaper with a dual-layer liquid crystal modulator [18] is used to compensate the extra anomalous dispersion of the lead-out fiber of FMLL in obtaining the transform-limited pulsewidth. The photomultiplier tube and the lock-in amplifier are used to measure the autocorrelation trace of the output pulsewidth when the heating temperature of SPEF is changed. When the cutoff wavelength of SPEF starts to overlap the spectral components of the mode-locked pulses from the long-wavelength end, the large negative dispersion is introduced into the laser cavity. The FMLL is moving from the anomalous dispersion regime to normal dispersion regime. The dispersion and Kerr nonlinearity in FMLL cannot be balanced to maintain the fixed pulsewidth. Consequently, the mode-locked pulses are stretched and are not transform-

limited. Also, the time-bandwidth product increases with the blue-shift of cutoff wavelength of SPEF.

### 3. Results and discussions

In the experiments, the EDF is backward pumped by a 122-mW 980-nm diode laser with a broadband ASE covering C+L band and partial S-band with the gain peak around 1.531  $\mu\text{m}$ . The total cavity length is estimated to be 10.2 m and the repetition rate of the femtosecond fiber laser is 20 MHz, measured by a radio-frequency (RF) spectrum analyzer. The average laser output power is 1.84 mW while the pulse energy is 0.092 nJ. The influence of cavity dispersion tailoring on pulse stretching is the key issue to be investigated in this work and thus the output power and pulse energy are not intentionally improved. In the beginning, the heating temperature of the liquid in SPEF was tuned to 36°C to obtain the shortest pulsewidth. The temperature is then gradually decreased. When the cutoff wavelength of SPEF is tuned to cut some of the long wavelength portions of the mode-locked pulses, as shown in Fig. 2(a), the net cavity dispersion is tuned to the normal dispersion regime and the pulsewidth is broadened. In Fig. 2(b), the experimental intensity auto-correlation traces show that pulsewidth at 36°C is 176.8fs (assuming a Gaussian pulse shape) and is gradually stretched to 269.4fs, 374.1fs, and 623.8fs at 35°C, 33°C, and 32°C, respectively. The polarization controller is fixed all the way to maintain the original eigen-states of longitudinal modes for the spectral components of mode-locked pulses. The temperature variation of 4°C on the SPEF can efficiently stretch the pulsewidth over the amount of 447fs (176.8-623.8fs), as shown in Fig. 2(b). The corresponding pulse stretch ratio is 3.53 (623.8/176.8). Clearly, the SPEF with a high cutoff slope can provide a large negative dispersion for the laser cavity. From Fig. 2(a), the laser output power slightly decreases when the cutoff wavelength of SPEF blue-shifts to cut some of the long wavelength tails of the gain bandwidth. However, the spectral gain profile of the FMLL is not significantly altered until the temperature is tuned to 32°C. The gain profile is substantially squeezed toward the shorter wavelengths at 32°C since a huge loss of higher than 30 dB, as can be seen from Fig. 1(b), is introduced by the SPEF closing to the central wavelength of mode-locked pulses. When the temperature is tuned below 32°C, the mode-locking is stopped because of the new center wavelength walks off too much and cannot fit well with the original mode-locking conditions. Moreover, the laser power could also be lower than the threshold power for maintaining the nonlinear Kerr effect. The time-bandwidth product is shown in Fig. 2(c). Clearly, the product increases with decreasing temperature at the SPEF since the FMLL is operated in the normal dispersion regime. The RF spectrum of the FMLL is shown in Fig. 2(d) and is steady with varying heating temperatures at SPEF. The RF spectra were measured at a room temperature of 22°C and the FMLL is placed on an aluminum plate with a plastic shielding to avoid the environment instability. The input pump power is 122-mW at 980-nm wavelength and the polarization controller is fixed all the way since the pulsewidth of 176.8 fs is achieved. In Fig. 2(d), the amplitude fluctuation is highly related to the pump power. A higher pump power can result in a more serious amplitude fluctuation due to the bleaching of absorber where the most intensive fluctuation peaks are compressed and amplified faster than the weaker peaks [19]. For the experiments in the control group, a SPEF with an inferior (not as sharp) cutoff slope is also employed in FMLL to investigate the pulse stretching but the results are poor. It is obvious that a steep cutoff slope filtering curve is crucial to an efficient cavity dispersion tailoring for a widely tunable pulse stretchable FMLL and no obvious walk-off for the center wavelength is observed before the mode-locking is stopped. The intra-cavity power and the amount of center wavelength walk-off are both the limiting factors for this pulse stretchable FMLL under the stationary mode-locking conditions. Accordingly, employing the multi-stage SPEFs in the laser cavity of FMLL is thus highly promising for the pulse stretching from the femtoseconds to the picoseconds in future works.

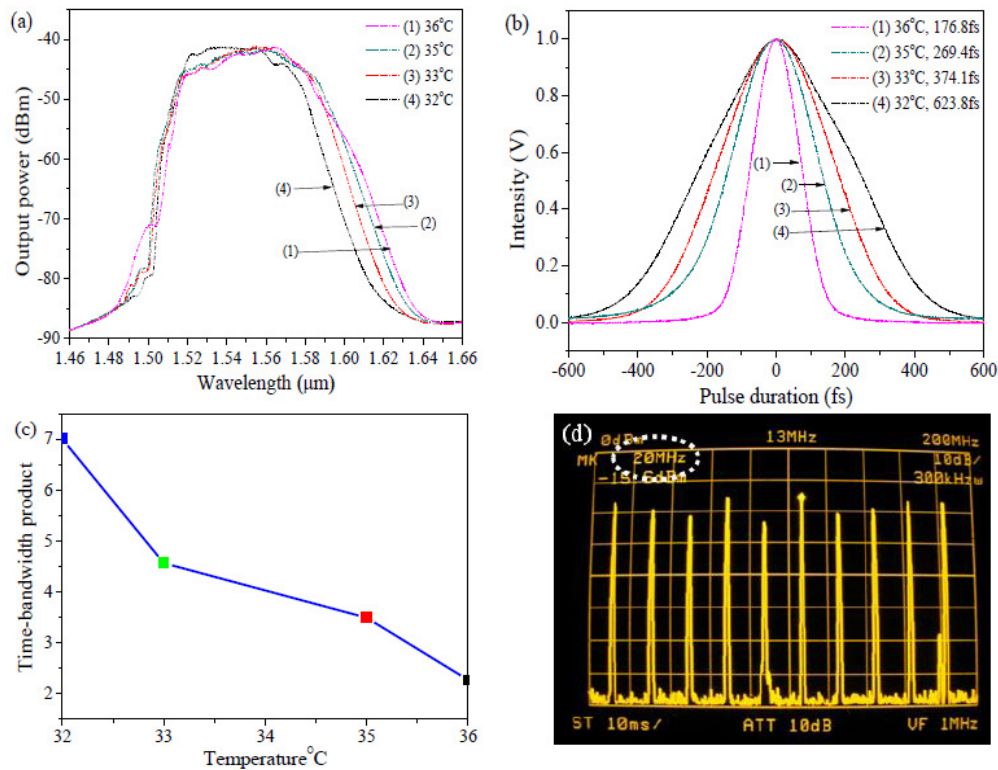


Fig. 2. (a) Output spectra of Er<sup>3+</sup>-doped mode-locked fiber laser with the SPEF operating at different temperatures (Res: 1 nm). (b) Pulse duration of the output pulses at different temperatures (assuming a Gaussian pulse shape). (c) Time-bandwidth product at different temperatures. (d) RF spectrum of the mode-locked laser.

#### 4. Conclusion

We have demonstrated pulse stretchable FMLL by incorporating a widely tunable SPEF into the laser ring cavity. The SPEF with a steep cutoff slope can introduce a large negative dispersion to tune the cavity dispersion from anomalous dispersion to normal dispersion regime. The corresponding pulsewidth of the output pulses can be stretched from 176.8fs to 623.8fs under a temperature variation of 4°C, without the need to change any fiber length. This approach enables the all-fiber femtosecond laser, to be efficiently pulse stretchable. This all-fiber scheme is simple, cost-effective, and wide-range tuning. The multistage intracavity SPEFs in laser cavity could be promising for achieving efficient pulse stretching to even large values for mode-locked fiber laser applications.

#### Acknowledgments

This work was supported in part by the R.O.C. National Science Council under Grants NSC 98-2221-E-239-001-MY2, NSC 100-2622-E-239-002-CC3, NSC 99-2628-E-018-013 and NSC 97-2923-E-011-001-MY3.